

# Lagrangian intermittencies in dynamic and static turbulent velocity fields from direct numerical simulations

E. LÉVÊQUE<sup>†</sup>, \*, L. CHEVILLARD<sup>†</sup>, <sup>‡</sup>, J.-F. PINTON<sup>†</sup>, S. ROUX<sup>†</sup>, A. ARNÉODO<sup>†</sup>  
and N. MORDANT<sup>†</sup>, <sup>§</sup>

<sup>†</sup>Laboratoire de physique, CNRS, École normale supérieure de Lyon, 46 Allée d'Italie,  
F-69364 Lyon cedex 7, France

<sup>‡</sup>Mechanical Engineering, The Johns Hopkins University, 3400 N. Charles Street,  
Baltimore, MD 21218, USA

<sup>§</sup>Laboratoire de physique statistique, CNRS, École normale supérieure de Paris 24 rue Lhomond,  
F-75005 Paris, France

Three temporal velocity signals are analyzed from direct numerical simulations of the Navier–Stokes (N–S) equations. The three signals are: (i) the velocity of fluid particles transported by the time-evolving solution (Eulerian velocity field) of the N–S equations, referred to as *the dynamic case*; (ii) the velocity of fluid particles transported by a solution of the N–S equations at some fixed time, referred to as *the static case*; and (iii) the time evolution of the solution of the N–S equations at some fixed positions, referred to as *the Eulerian case*. The comparison of these three signals aims at elucidating the importance of the overall spacetime evolution of the flow on Lagrangian statistics. It is observed that the static case is, to some extent, similar to the Eulerian case; a feature that can be understood as an ergodicity property of homogeneous and isotropic turbulence and can be related to the process of random sweeping. The dynamic case is clearly different. It bears the signature of the time evolution of the flow. This study emphasizes the importance of the global dynamics of the flow and points out the existence of long-time correlations in the fluid-particle dynamics in the Lagrangian description.

## 1. Introduction

### 1.1 *The motivations*

In a recent past, a significant effort has been devoted to the description of fluid-particle (or Lagrangian) accelerations in fully turbulent flows [1–3]. These approaches are mainly rooted in the idea of modeling the fluid-particle dynamics by an equation of Langevin type (by analogy to the Brownian motion), where the stochastic force would represent the stirring action of turbulence on the particle (see [4] for a comparative analysis of one-dimensional Langevin models). If the stirring force is assumed uncorrelated in time, the statistics of the (one-dimensional) Lagrangian velocity is mono-fractal with a similarity exponent equal to  $1/2$ —the velocity structure functions scale as  $\langle |v(t + \tau) - v(t)|^p \rangle \sim \tau^{p/2}$  for all  $p$ . This corresponds to the non-intermittent Kolmogorov's picture [5]. Experimental and numerical studies have provided the evidence of intermittency [6, 7]. The scaling exponents deviate from the (linear) scaling law  $p/2$ . Intermittency implies that multi-time correlations should be ascribed to

---

\*Corresponding author. E-mail: Emmanuel.Leveque@ens-lyon.fr

the turbulence-stirring force. Accordingly, it has been proposed to model the trajectory of a fluid particle by a ‘multifractal random walk’ [8], in which the force exhibits a random direction but a long-range correlated magnitude. This phenomenological model, in which long-time correlations and the occurrence of large amplitude events at small scales dominate the motion, suitably accounts for the multifractal properties of the Lagrangian velocity [6–8]. The underlying picture is that a fluid particle, along its trajectory, encounters intense vortical structures (and sometimes gets trapped for a significant amount of time [9]) over a quiescent background Eulerian velocity field. Within this picture, Lagrangian intermittency is linked to the nature, the distribution and the time evolution of the dynamical structures embedded in the flow. In order to better understand the importance of the spacetime evolution of the flow, we propose to examine and compare three different temporal velocity signals obtained from direct numerical simulations (section 1.2) [10]. The energy spectra, the scaling behavior of Lagrangian velocity structure functions and the correlations in time of velocity increments are investigated.

Another argument in favor of the importance of the overall dynamics may be put forward as follows. The turbulence-stirring force is associated with the negative pressure gradient at the location of the fluid particle (neglecting dissipative effects at inertial time scales). From the Navier–Stokes equations, the pressure is the solution of a Poisson (elliptic) equation, with the divergence of  $(\mathbf{u} \cdot \nabla)\mathbf{u}$  as a source term [11]. It is thus expected that the overall distribution of velocity gradients (over the whole domain) influences the pressure at a particular position. This reasoning emphasizes again the plausible importance of the whole flow on the fluid-particle dynamics.

## 1.2 The three temporal velocity signals

Three velocity signals  $\mathbf{v}(t)$  are examined;  $\mathbf{v}(t)$  is the value, at time  $t$ , of the Eulerian velocity field  $\mathbf{u}(\mathbf{x}, t)$  at some observation point  $\mathbf{x}(t)$ :

$$\mathbf{v}(t) = \mathbf{u}(\mathbf{x}(t), t).$$

Three cases are considered.

- (i) The *dynamic case*, which pertains to the fluctuations in time of the velocity of marked fluid particles:

$$\dot{\mathbf{x}}(t) = \mathbf{u}(\mathbf{x}(t), t),$$

where  $\mathbf{u}(\mathbf{x}, t)$  is the time-evolving solution of the Navier–Stokes equations.

- (ii) The *frozen case*:

$$\dot{\mathbf{x}}(t) = \mathbf{u}(\mathbf{x}(t), t_0),$$

where  $\mathbf{u}(\mathbf{x}, t_0)$  is a frozen (in time) solution of the Navier–Stokes equations. A single snapshot of a converged turbulent flow is used to advect the fluid particles.

- (iii) The *Eulerian case*:

$$\mathbf{v}(t) = \mathbf{u}(\mathbf{x}_0, t).$$

The velocity is recorded at some fixed spatial points in the computational domain, as it would be measured by local probes in a real turbulent flow. Considered here is the case where turbulence develops in the absence of a mean flow; otherwise the Taylor frozen turbulence hypothesis states that the turbulent structure is advected past the measuring probe at the mean flow speed, and time measurements trivially reduce to spatial

Table 1. The parameters and Eulerian characteristic scales of the simulations.

	grid	$u_{\text{rms}}(\text{m s}^{-1})$	$\nu (\text{m}^2\text{s}^{-1})$	$\varepsilon (\text{m}^2\text{s}^{-3})$	$\eta (\text{m})$	$\lambda (\text{m})$	$R_\lambda$	$L (\text{m})$
run1	128 <sup>3</sup>	0.12	5.4 10 <sup>-4</sup>	1.0 10 <sup>-3</sup>	0.020	0.34	75	0.84
run2	256 <sup>3</sup>	0.12	1.5 10 <sup>-4</sup>	1.0 10 <sup>-3</sup>	0.0075	0.18	140	0.75

$u_{\text{rms}}$  is the root-mean-square velocity,  $\nu$  the kinematic viscosity,  $\varepsilon$  the mean dissipation,  $\eta \equiv (\nu^3/\varepsilon)^{1/4}$  the Kolmogorov's dissipative scale,  $\lambda \equiv \sqrt{15\nu u_{\text{rms}}^2/\varepsilon}$  the Taylor micro-scale and  $R_\lambda \equiv u_{\text{rms}}\lambda/\nu$  is the turbulent Reynolds number.  $L = (\pi/2) \int k^{-1} E(k) dk / u_{\text{rms}}^2$  is the estimate of the (longitudinal) integral scale, where  $E(k)$  denotes the mean energy spectrum in wavenumber.

measurements. The Eulerian temporal velocity statistics in the absence of mean flow is more controversial [13, 14].

To what extent does the statistics of (one-dimensional) velocity increments  $\delta v(\tau) \equiv v_x(t + \tau) - v_x(t)$  depend on the case under investigation?

### 1.3 The numerical tools

The three cases are examined numerically.

The N–S equations are solved in a cubic domain with periodic boundary conditions, using a parallel distributed-memory pseudo-spectral solver (without de-aliasing). The time integration is performed by a (second order in time) leap-frog scheme. In order to sustain a (statistically) stationary state, a large-scale forcing is supplied to the dynamics, so as to compensate exactly the losses due to molecular dissipation; in other words, the total kinetic energy of the system is kept constant. This robust and efficient forcing scheme permits a rapid relaxation to stationarity.

The trajectories of fluid particles are discretized in time by a second-order Runge–Kutta scheme:

$$x^{n+1} = x^n + \frac{\Delta t}{2} \left[ u^n(x^n) + u^{n+1}(x^n + \Delta t u^n(x^n)) \right].$$

The velocity of a particle is interpolated from the nodal values of the Eulerian velocity field, using cubic spline functions [12]. In the dynamic and static cases,  $10^4$  particles have been followed during approximately  $5T_L^*$ , where  $T_L^*$  is the correlation time of the particle velocity. At this point, it should be noted that the Lagrangian integral time  $T_L$  (computed as the integral of the Lagrangian velocity correlation function) notably underestimates the value of the correlation time  $T_L^*$  for which  $\langle v(T_L^*)v(0) \rangle \approx 0$  (see figure 1). This feature implies that a satisfactory convergence of Lagrangian velocity statistics actually requires a simulation over a time interval much larger than the Lagrangian integral time. The choice of a rather *low-resolution* simulation was here primarily dictated by the fulfilment of this convergence requirement.

Finally, the parameters and characteristic times of the simulations are reported in tables 1 and 2. Let us mention that run1 was exploratory, numerical results have been computed from run2.

Table 2. The Eulerian and Lagrangian (for the dynamic case) characteristic times of the simulations.

	$R_\lambda$	$T_E(\text{s})$	$T_L(\text{s})$	$T_L^*(\text{s})$	$t_\eta(\text{s})$	$dt(\text{s})$
Run1	75	6.9	5.9	$\sim 25$	0.74	0.025
Run2	140	6.2	4.8	$\sim 20$	0.39	0.005

$T_E \equiv L/u_{\text{rms}}$  is the integral-scale eddy turn-over time,  $T_L$  the (usual) Lagrangian integral time,  $T_L^*$  is the Lagrangian correlation time and  $t_\eta \equiv (\nu/\varepsilon)^{1/2}$  the Kolmogorov's dissipative time.  $dt$  is the time step of the numerical integration.

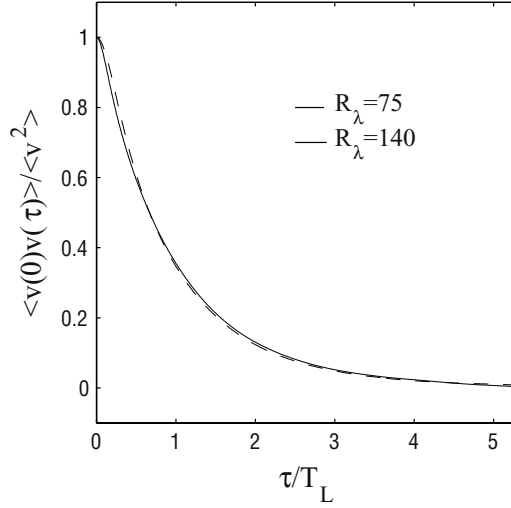


Figure 1. The Lagrangian correlation time  $T_L^*$  for which  $\langle v(T_L^*)v(0) \rangle \approx 0$  is much larger than the Lagrangian integral time  $T_L$ . The existence of long-time correlations in the Lagrangian velocity imposes that numerical simulations should be run over time intervals much larger than  $T_L$ . In the present simulations, the statistics have been sampled over about  $20T_L$ .

## 2. Frequency energy spectra

Firstly, the focus is on two-time velocity correlations. The mean energy spectrum versus frequency is plotted in figure 2 for the three cases. All spectra exhibit a power-law scaling but with different slopes. The corresponding local exponents, determined from the local logarithmic slope of spectra, are displayed in the inset.

On the one hand, the dynamic frequency spectrum exhibits a scaling behavior close to  $\omega^{-2}$ , as predicted from Kolmogorov's similarity arguments [13] and already reported in literature:

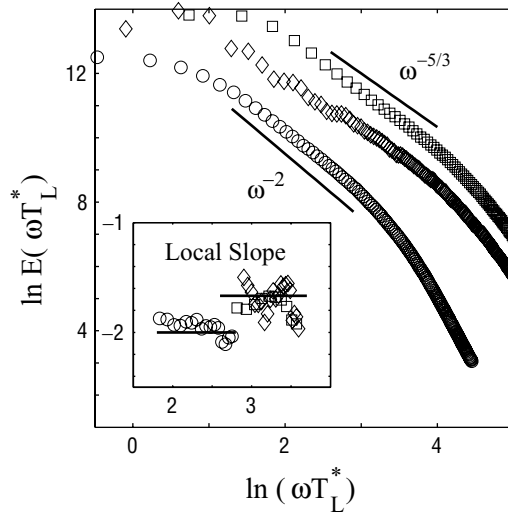


Figure 2. Spectra of energy in frequency of one component of the velocity of fluid particles evolving in the dynamic case (O), the static case ( $\square$ ) and the Eulerian case ( $\diamond$ ).  $T_L^*$  denotes the correlation time for each signal. Spectra have been shifted for clarity.

$E(\omega) = \varepsilon \omega^{-2} f(\omega/\omega_0)$  with the Lagrangian dissipative frequency  $\omega_0 = (\varepsilon/\nu)^{1/2}$  (stemming from dimensional analysis). On the other hand, the static and Eulerian frequency spectra show a scaling exponent closer to  $-5/3$ , characteristic of the Eulerian spectrum in wavenumber. This exponent is consistent with Tennekes's random-sweeping argument [14]. Small-scale eddies are randomly swept without distortion, with a characteristic velocity  $u_{\text{rms}}$  past the observation point  $\mathbf{x}(t)$ —in the frame of reference attached to  $\mathbf{x}(t)$ . Indeed, it follows from this assumption that the spectrum in frequency  $E(\omega)$  is given by the spectrum in wavenumber  $E(k) = \varepsilon^{2/3} k^{-5/3} f(k\eta)$ , where  $\eta = (\nu^3/\varepsilon)^{1/4}$ , with the identification  $\omega = k u_{\text{rms}}$ :

$$E(\omega) = \varepsilon^{2/3} u_{\text{rms}}^{2/3} \omega^{-5/3} f\left(\frac{\omega}{\omega_c}\right).$$

The cut-off frequency is  $\omega_c = u_{\text{rms}}/\eta$ , which may be written as  $\omega_c \simeq 0.5 \omega_0 R_\lambda^{1/2}$ , where  $R_\lambda = u_{\text{rms}}\lambda/\nu$  is the Reynolds number based on the Taylor micro-scale  $\lambda = \sqrt{15\nu u_{\text{rms}}^2/\varepsilon}$ . The cut-off frequency of the sweeping process is therefore much larger than the Lagrangian dissipative scale  $\omega_0$ . This produces a wider inertial range as evidenced in figure 2. Let us note that such discrepancies between Eulerian wavenumber and Eulerian frequency spectra had already been reported in [16].

The  $\omega^{-5/3}$  scaling observed for the static case is at first sight surprising, even if this scaling had also been observed in a similar study using *kinematic simulations* [18]. In the static case,  $\dot{\mathbf{v}} = \partial_t \mathbf{u} + (\dot{\mathbf{x}} \cdot \nabla) \mathbf{u}$  with  $\partial_t \mathbf{u} = \mathbf{0}$  and  $\dot{\mathbf{x}} = \mathbf{u}$ . This yields for the particle acceleration  $\dot{\mathbf{v}} = (\mathbf{u} \cdot \nabla) \mathbf{u}$  and for the variance  $\langle |\dot{\mathbf{v}}|^2 \rangle = \langle |(\mathbf{u} \cdot \nabla) \mathbf{u}|^2 \rangle$ . Here, the average is meant on time along the trajectory. The hypothesis of random sweeping (small-scale velocity gradients are swept by the large-scale velocities without distortion) implies that

$$\langle |\dot{\mathbf{v}}|^2 \rangle_{\text{static}} \approx \langle |\mathbf{u}|^2 \rangle \langle |\nabla \mathbf{u}|^2 \rangle \sim u_{\text{rms}}^2 \varepsilon \nu^{-1},$$

which grows more rapidly than the Lagrangian estimate:

$$\langle |\dot{\mathbf{v}}|^2 \rangle_{\text{dynamic}} = \varepsilon^{3/2} \nu^{-1/2}$$

with the Reynolds number [15].

These first results emphasize the importance of the time evolution of the flow ( $\partial_t \mathbf{u}(\mathbf{x}, t) \neq \mathbf{0}$ ) on two-time statistics and in particular on the acceleration variance.

### 3. Intermittency characteristics

We now seek to quantify the intermittency features of the velocity fluctuations. This is usually achieved via the analysis of the so-called velocity structure functions  $\langle |\delta v(\tau)|^p \rangle$  as functions of the scale  $\tau$ , and it is expected that velocity structure functions exhibit power-law scalings in the inertial range:

$$\langle |\delta v(\tau)|^p \rangle \sim \tau^{\zeta_p}.$$

Intermittency refers to the nonlinear behavior of  $\zeta_p$  in  $p$ .

As already advocated in [17], the cumulant expansion provides an alternative, physically sound description of the scaling properties of velocity fluctuations:

$$\log \langle |\delta v(\tau)|^p \rangle = p C_1(\tau) + \frac{p^2}{2} C_2(\tau) + \frac{p^3}{6} C_3(\tau) + \dots,$$

where  $C_p(\tau)$  represents the  $p$ th-order cumulant of  $\log |\delta v(\tau)|$ . In the inertial range, every  $C_p(\tau)$  is expected to behave as a linear function of  $\log(\tau)$ :  $C_1(\tau) = c_1 \log \tau$ ,  $C_2(\tau) = -c_2 \log \tau$ , etc., and the scaling exponents  $\zeta_p$  are given by Taylor's expansion  $\zeta_p = \sum_{k=1}^{\infty} c_k (-1)^{k+1} p^k / k!$ .

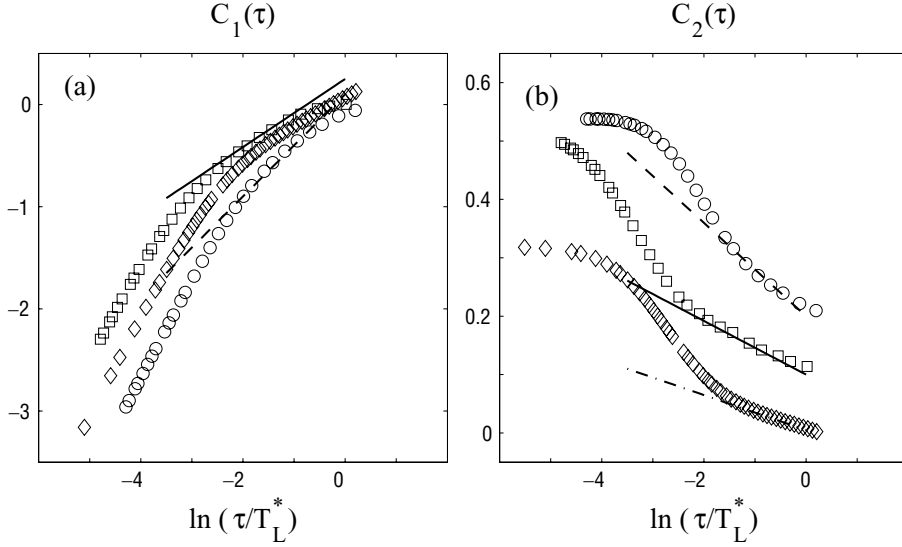


Figure 3. The first two cumulants of velocity amplitudes for the dynamic case (O), the static case (□) and the Eulerian case (◇). (a): the dash and solid lines correspond to the slopes  $c_1 = 1/2$  and  $c_1 = 1/3$ , respectively. (b): the dashed, solid and dashed-dotted lines correspond to the slopes  $c_2^{\text{dynamic}} = 0.08$ ,  $c_2^{\text{static}} = 0.046$  and  $c_2^{\text{Eulerian}} = 0.03$ .

In a sense, the previous cumulant expansion allows us for a perturbative approach of intermittency. Indeed, if only the first-order cumulant is retained in the expansion, (non-intermittent) Kolmogorov's theory (for Lagrangian velocity increments) is obtained with  $c_1 = 1/2$ ; the log-normal assumption is recovered by retaining only the first two terms in expansion and

$$\zeta_p = c_1 p - c_2 \frac{p^2}{2},$$

and so on. For our purpose, we will focus on the first two cumulants.

The behavior of  $C_1(\tau)$  and  $C_2(\tau)$  for the dynamic, static and Eulerian cases are reported in figure 3. For the dynamic case,  $C_1(\tau) \approx 1/2 \log(\tau/T_L^*)$  in agreement with the  $(\omega T_L^*)^{-2}$  scaling observed in the inertial range for the energy spectrum. In contrast, the first-order cumulant for the static and Eulerian cases is better approximated by  $C_1(\tau) \approx 1/3 \log(\tau/T_L^*)$ . This scaling exponent is again consistent with the  $(\omega T_L^*)^{-5/3}$  behavior observed for the energy spectra. The second-order cumulant exhibits also a logarithmic behavior (in the inertial range). For the dynamic case,  $C_2(\tau) \approx -0.08 \log(\tau/T_L^*)$  in good agreement with previous experimental data [6] and numerical simulations [7]. For the static and the Eulerian cases,  $C_2(\tau) \approx -0.046 \log(\tau/T_L^*)$  and  $C_2(\tau) \approx -0.03 \log(\tau/T_L^*)$ , respectively. These exponents may be compared to the intermittency coefficient  $c_2 = 0.049 \pm 0.003$  computed numerically from the wavelet decomposition of three-dimensional Eulerian velocity fields [19] and to the value  $c_2 = 0.025 \pm 0.003$  obtained from one-dimensional Eulerian longitudinal velocity increments [17]. We may thus conclude that the static and Eulerian cases have similar statistics to, respectively, the three-dimensional and one-dimensional Eulerian velocity fields, while the dynamic case is clearly more intermittent. This is confirmed in figure 4, where the relative scaling exponents are displayed and compared. Another puzzling feature reported in figure 4 is the similarity between the relative scaling exponents of passive scalar increments [20–21] and those of Lagrangian velocity increments (within error bars).

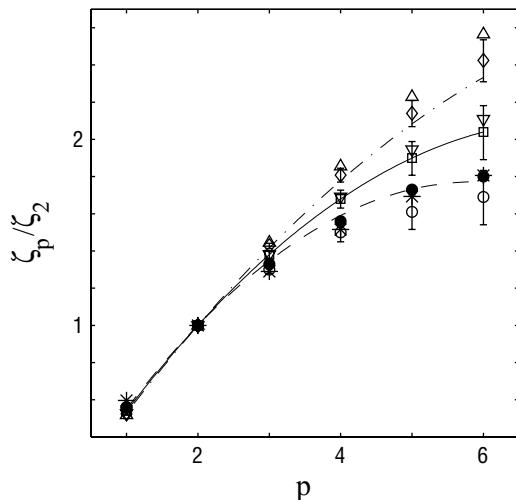


Figure 4. The relative scaling exponents  $\zeta_p/\zeta_2$  computed for the dynamic case (O), the static case (□) and the Eulerian case (◇). For comparisons, the exponents obtained from experimental measurements of Lagrangian velocity increments (•), the wavelet decomposition of three-dimensional Eulerian velocity fields (∇), one-dimensional Eulerian longitudinal velocity increments (Δ), and passive scalar increments (★).

#### 4. Long-time correlations

A characteristic property of turbulent Lagrangian dynamics is the observation of long-time correlations [8]. This refers to the fact that acceleration and velocity increments are rapidly decorrelated in time (because of the fluctuation of their direction, with a frequency comparable to  $\omega_0$ ), while their magnitude remains correlated over a time interval of the order of  $T_L^*$  (the correlation time of the Lagrangian velocity). In order to better quantify this phenomenon and compare our three velocity signals, we introduce the magnitude-connected correlation function [8, 17]:

$$\chi_\tau(\Delta t) = \langle \ln |\delta v(t, \tau)| \ln |\delta v(t + \Delta t, \tau)| \rangle - \langle \ln^2 |\delta v(t, \tau)| \rangle, \quad (1)$$

where  $\delta v(t, \tau) = v(t + \tau) - v(t)$  denotes the Lagrangian velocity increment (over a time scale  $\tau$ ) at time  $t$ .

The numerical estimation of  $\chi_\tau(\Delta t)$  is plotted in figure 5 as a function of  $\ln(\Delta t/T_L^*)$  for our three velocity signals. For each signal, the time scale  $\tau$  was set to be the smallest inertial time scale (for which dissipative effects remain negligible) and the time interval  $\Delta t$  was considered greater than or equal to  $\tau$  (in order to avoid overlap between successive increments). As a matter of fact, the first point of each plot (on the left) corresponds to  $\Delta t = \tau$ . With the help of figure 3(b),  $\tau$  may be roughly seen as the smallest scale for which  $C_2(\tau)$  remains proportional to  $\ln \tau$ , and thus, may be considered as the smallest inertial time scale. A first striking observation is that all  $\chi_\tau(\Delta t)$  vanish at  $\Delta t$  very close to  $T_L^*$ , stating that for the three cases, magnitudes of inertial velocity increments are long-range correlated. Furthermore, it is also observed in figure 5 that the three correlation functions  $\chi_\tau(\Delta t)$  behave linearly with respect to  $\ln \Delta t$  (the issue of possible quadratic corrections is addressed in [22]), with the same slopes as the corresponding second-order cumulants (see figure 3(b)). This latter feature suggests that, in each case, a similar (underlying) multi-time mechanism relates intermittency to the long-time correlations of velocity increments. This mechanism may be considered as a random multiplicative cascade, as originally proposed by Cates and Deutsch [23] (see also [8, 17, 22]).

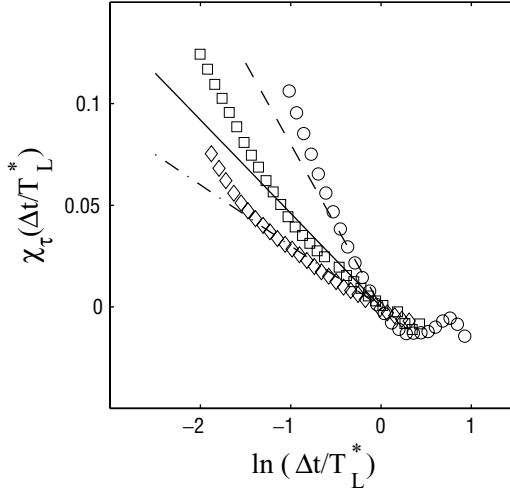


Figure 5. Estimation of the magnitude-connected correlation function  $\chi_\tau(\Delta t)$  as a function of the time lag  $\Delta t/T_L^*$ , in the dynamic case ( $\circ$ ), the static case ( $\square$ ) and the Eulerian case ( $\diamond$ ). The first points of each plot (on the left) are such that  $\Delta t = \tau$ , which allows us to read  $\tau$  directly on the axis (and compare with figure 3.). The straight lines have the same slopes as in figure 3(b).

Thus, statistics obtained from the three velocity signals point out unambiguously the existence of an underlying cascade (with different slopes according to each case) which correlates the amplitudes of Lagrangian velocity increments at any small scales with the global dynamics of flow, i.e., the dynamics over a period of time comparable to  $T_L^*$ . This feature again insists on the importance of the dynamics of the flow in the fluid-particle dynamics.

## 5. Conclusion

It is found that velocity fluctuations of particles advected by a frozen Eulerian velocity field are, to some extent, similar to the fluctuations in time of the Eulerian velocity field at some fixed points. In both cases, the acceleration  $\dot{\mathbf{v}}(t)$  is dominated by the nonlinear term  $(\mathbf{u} \cdot \nabla)\mathbf{u}$  at the observation point  $\mathbf{x}(t)$ ; a feature which may be related to the phenomenon of random sweeping. In the static case, the velocity field  $\mathbf{u}(\mathbf{x}, t)$  is frozen in time but  $\mathbf{x}(t)$  explores the whole domain, while in the Eulerian case, the velocity field  $\mathbf{u}(\mathbf{x}, t)$  evolves in time but  $\mathbf{x}(t)$  is fixed. The similarity between the static and the Eulerian cases may therefore be understood as an ergodicity property of homogeneous (without mean flow) and isotropic turbulence. Finally, the intermittency measured in the dynamic case is very different. The present results indicate that fluid particle dynamics are indeed very sensitive to the global time evolution of the flow; a feature that may indicate that non-homogeneous large-scale dynamics of the flow should be taken into account explicitly in the modeling of Lagrangian dynamics.

## Acknowledgement

This work has been supported by the French Minist  re de la recherche and the Centre National de la Recherche Scientifique. Numerical simulations have been performed at the CINES (France) using an IBM SP4 computer.



## References

- [1] Voth, G. A., La Porta, A., Crawford, A. M., Alexander, J. and Bodenschatz, E., 2002, Measurement of particle accelerations in fully developed turbulence. *Journal of Fluid Mechanics*, **469**, 121–160.
- [2] Mordant, N., Crawford, A. M. and Bodenschatz, E., 2004, Three-dimensional structure of the Lagrangian acceleration in turbulent flows. *Physical Review Letters*, **93**(21), 214501.
- [3] Yeung, P. K., 2002, Lagrangian investigations of turbulence. *Annual Review of Fluid Mechanics*, **34**, 115–42.
- [4] Aringazin, A.K. and Mazhitov, M.I., 2004, One-dimensional Langevin models of fluid particle acceleration in developed turbulence. *Physical Review E*, **69**(2), 026305.
- [5] Monin, A. M. and Yaglom, A. S., 1987, *Statistical Fluid Mechanics*. (Cambridge, MA: MIT Press)
- [6] Chevillard, L., Roux, S. G., L ev eque, E., Mordant, N., Pinton, J.-F. and Arn odo, A., 2003, Lagrangian velocity statistics in turbulent flows: effect of dissipation. *Physical Review Letter*, **91**(21), 214502.
- [7] Biferale, L., Boffetta, G., Celani, A., Devenish, B. J., Lanotte, A. and Toschi, F., 2004, Multifractal statistics of Lagrangian velocity and acceleration in turbulence. *Physical Review Letters*, **93**(6), 064502.
- [8] Mordant, N., Delour, J., L ev eque, E., Arn odo, A. and Pinton, J.-F., 2002, Long-time correlations in Lagrangian dynamics: A key to intermittency in turbulence. *Physical Review Letters*, **89**, 254502.
- [9] Biferale, L., Boffetta, G., Celani, A., Lanotte, A. and Toschi, F., 2005, Particle trapping in three-dimensional fully developed turbulence. *Physics of Fluids*, **17**(2), 021701.
- [10] Chevillard L., Roux S. G., Leveque E., Mordant N., Pinton J.-F. and Arneodo A., 2005, Intermittency of velocity time increments in turbulence. *Physical Review Letters*, **65**(6), 064501.
- [11] Frisch, U., 1995, Turbulence: *The Legacy of A. N. Kolmogorov* (Cambridge, UK: Cambridge University Press).
- [12] Yeung, P. K. and Pope, S. B., 1989, Lagrangian statistics from direct numerical simulations of isotropic turbulence. *Journal of Fluid Mechanics*, **207**, 531–586.
- [13] Tennekes, H. and Lumley, J. L., 1972, *A First Course in Turbulence*. (Cambridge, MA: MIT Press).
- [14] Tennekes, H., 1975, Eulerian and Lagrangian time microscales in isotropic turbulence. *Journal of Fluid Mechanics*, **67**, 561–567.
- [15] Nelkin, M. and Tabor, M., 1989, Time correlations and random sweeping in isotropic turbulence. *Physics of Fluids A*, **2**(1), 81–83.
- [16] Yeung, P. K. and Sawford B. L., 2002, Random-sweeping hypothesis for passive scalars in isotropic turbulence. *Journal of Fluid Mechanics*, **459**, 129–138.
- [17] Delour, J., Muzy, J.-F. and Arn odo, A., 2001, Intermittency of 1d velocity profiles in turbulence: A magnitude cumulant analysis. *European Physics Journal B*, **23**(2), 243–248.
- [18] Khan, M. A. I. and Vassiliocs, J. C., 2004, A new Eulerian–Lagrangian length-scale in turbulent flows. *Physics of Fluids*, **16**(1), 216–218.
- [19] Kestener P. and Arn odo, A., 2004, Generalizing the wavelet-based multifractal formalism to random vector fields: Application to three-dimensional turbulence velocity and vorticity data. *Physical Review Letter*, **93**(4), 044501.
- [20] Ruiz-Chavarr a, G., Baudet, C. and Ciliberto, S., 1995, Extended self-similarity of passive scalars in fully-developed turbulence. *Europhysics Letters*, **32**(4), 319–324.
- [21] Chen, S. and Cao, N., 1997, Anomalous scaling and structure instability in three-dimensional passive scalar turbulence. *Physical Review Letters*, **78**(18), 3459–3462.
- [22] Castaing, B., 2002, Lagrangian and Eulerian velocity intermittency. *European Physics Journal B*, **29**, 357–358.
- [23] Cates, M.E. and Deutsch, J.M., 1987, Spatial correlations in multifractals. *Physical Review A*, **35**, 4907–4910.